Journal of Molecular Catalysis B: Enzymatic 72 (2011) 130–138

Contents lists available at ScienceDirect

Journal of Molecular Catalysis B: Enzymatic

journal homepage: www.elsevier.com/locate/molcatb

Probing a family GH11 endo-β-1,4-xylanase inhibition mechanism by phenolic compounds: Role of functional phenolic groups

Imen Boukari[a,b], Michael O'Donohue[c,d,e], Caroline Rémond[a,b], Brigitte Chabbert[a,b,*]

[a] INRA, UMR614, Fractionnement des AgroRessources et Environnement, F-51100 Reims, France
[b] University of Reims Champagne Ardenne, UMR614, Fractionnement des AgroRessources et Environnement, F-51100 Reims, France
[c] Université de Toulouse; INSA, UPS, INP, LISBP, F-31077 Toulouse, France
[d] INRA, UMR792 Ingénierie des Systèmes Biologiques et des Procédés, F-31400, France
[e] CNRS, UMR5504, F-31400 Toulouse, France

ARTICLE INFO

Article history:
Received 9 December 2010
Received in revised form 22 May 2011
Accepted 25 May 2011
Available online 1 June 2011

Keywords:
Inhibition
Lignin degradation products
Endoxylanase
Phenolic compounds

ABSTRACT

Phenolic compounds generated from lignin degradation during the pre-treatment step in the process of producing bioethanol from lignocellulosic biomass are known to be inhibitory to enzymatic hydrolysis and fermentation. The inactivation mechanism of a GH11 endoxylanase (Tx-Xyl) by several phenolic compounds varying in their hydroxyl and methoxyl radical content was investigated. Apparent kinetic inactivation parameters were measured as an approximate index of the inhibitory effects. All the tested aromatic compounds had strong negative impact on enzyme activity and kinetic analysis revealed non competitive multi-site inhibition mechanism. The interactions between Tx-Xyl and the phenolic compounds were further studied by steady-state (tryptophan) fluorescence spectroscopy. Changes in λ_{max} of emission and quenching of fluorescence intensity indicated changes in the microenvironment of tryptophan residues. In agreement with the kinetic parameters, the fluorescence derived binding constants evidenced higher enzyme–phenolics interaction affinity with increasing phenolic hydroxyl radical content, suggesting clear correlations of such radicals with the inhibitory effects. Results indicated that the inhibitory effects of phenolic compounds on Tx-Xyl activity are most likely brought about by conformational alterations of the enzyme protein inducing steric inactivation.

1. Introduction

Rising environmental and economic concerns linked to Man's dependency on fossil fuels are currently driving research and development aimed at the development of viable energy alternatives, such as ethanol, using biomass as a lignocellulosic feedstock. To attain this goal, it is necessary to design cost-efficient manufacturing processes that will allow both the production of ethanol from cellulose and hemicelluloses sugars and the optimal conversion of the hemicellulose and lignin components into other valuable products [1].

Currently, the basic concept for the production of ethanol from lignocellulosic biomass consists of several distinct steps, which includes biomass pretreatment, enzymatic hydrolysis and yeast-mediated fermentation [2–4]. Most enzymatic hydrolysis technologies employ enzyme cocktails including cellulases (endoglucanases, cellobiohydrolases, and β-glucosidases), hemicellulases (mainly endoxylanases), and/or lignin-degrading enzymes [5]. Recalcitrance of lignocelluloses to bioconversion is mainly due to their structural complexity, but also to their aromatic constituents which include both lignins and phenolic acids [6]. Thus, although pretreatment is a significant cost-driver, it is an indispensable step prior to enzymatic processes. Pretreatment disrupts the plant cell wall network, partially separates the major polymer components (lignin, cellulose and hemicellulose) and increases the accessibility of cellulose fibres to enzymes [7]. However, depending on the exact nature of the pretreatment, the consequences for the non-cellulose components are variable [8]. Frequently, pretreatment provides only partial degradation of the lignin component. Additionally, the non-specific conditions of pretreatment can lead to the generation of undesirable soluble by-products, such as furfurals and aromatics [9–11]. Along with residual lignins, these latter compounds are known to inhibit both the subsequent enzymatic hydrolysis and fermentation steps [9,12–14]. Therefore, the optimal removal or alteration of lignin and other aromatic biomass components, which are potentially valuable co-products of the biorefining process, is a key challenge to increase enzyme access to the polysaccharide components and,

Abbreviation: Tx-Xyl, endo-β-1,4-xylanase from *Thermobacillus xylanilyticus*.

* Corresponding author at: INRA, UMR614, FARE 2 Esplanade R. Garros, BP 224, 51100 Reims, France. Tel.: +33 3 26 77 35 94.
E-mail address: chabbert@reims.inra.fr (B. Chabbert).

1381-1177/$ – see front matter © 2011 Elsevier B.V. All rights reserved.
doi:10.1016/j.molcatb.2011.05.010

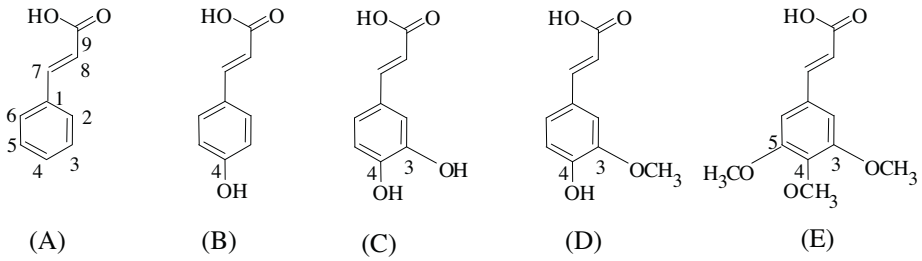

Fig. 1. Model phenolic compounds. (A) Cinnamic acid; (B) *p*-coumaric acid; (C) caffeic acid; (D) ferulic acid; and (E) 3,4,5-trimethoxy-cinnamic acid.

ultimately, to increase the efficiency and economics of lignocellulose conversion processes [15,16].

Undesirable pretreatment by-products include a wide range of phenolic monomers and oligomers derived from the cell wall phenolic acids such as ferulic acid and *p*-coumaric acid, and lignins [17–19]. Lignins are polymers composed of three basic subunits, hydroxyphenyl, guaiacyl, and syringyl moieties, which differ only with regard to the number of methoxyl substitutions of the aromatic ring (0, 1 and 2 respectively) [20,21]. During pre-treatment, cleavage of the intermonomer bonds results in the release of soluble mono- and oligo-aromatic compounds and an increase in the concentration of free phenolic radicals [19].

The effects of phenolic compounds on cellulose and hemicellulose-degrading glycoside hydrolases have been largely evidenced and documented in the literature. Sharma et al. [22] reported that guaiacol (2-methoxyphenol) and caffeic acid (3,4-dihydroxycinnamic acid) significantly inhibited the activity of a xylanase contained in crude extracts from *Aspergillus japonicus* [22]. Similarly, Senior et al. showed that compounds leaching from lignin in pulping liquors produced significant inhibition of a xylanase from *Trichoderma harzianum* [23]. Kaya et al. [24] found that some lignin degradation products present in alkaline spent pulping liquors, such as vanillic acid, protocatechuic acid, guaiacol and vanillin had varying effects on xylanase activity, depending on the exact concentration of these molecules. At low concentration, positive activation effects were measured, while at higher concentrations enzyme activity was lost [24]. Regarding cellulases, inhibition of commercial cellulase cocktails was evidenced in presence of steam-exploded softwood liquid fraction and vanillin, syringaldehyde, trans-cinnamic acid, and hydroxybenzoic acid [14,25].

Overall, despite proposals that phenolic hydroxyl groups might form a key element in the inhibition potency of lignin-derived aromatics towards enzymes [26,27], little is actually known about the nature of the interactions or of the inhibitory mechanisms. Therefore, the acquisition of new knowledge in this area is a prerequisite for the further optimisation of biorefining processes through the engineering of effective enzymatic treatment.

In the present study, the mechanism of inhibition of a GH11 endo-β-1,4-xylanase from *Thermobacillus xylanilyticus* by several phenolic compounds has been investigated. Kinetic analyses and a fluorescence spectrophotometric study provide insight into the nature and extent of the interactions between the enzyme and various phenolic compounds. Overall, our results procure new understanding of how hemicellulases might be inhibited in biorefining processes by lignin degradation products.

2. Materials and methods

2.1. Phenolic compounds and preparation of solutions

Five phenolic compounds were used as models of lignin degradation products (Fig. 1). Cinnamic acid (≥99.5%) (A), *p*-coumaric acid (4-hydroxycinnamic acid) (≥98%) (B), caffeic acid (3,4-dihydroxycinnamic acid) (≥99%) (C), ferulic acid (3-methoxy,4-hydroxycinnamic acid) (≥98%) (D) and 3,4,5-trimethoxycinnamic acid (≥98%) (E) were purchased from Sigma–Aldrich and used without further purification. Concentrated solutions (100 mM) of these compounds were prepared by dissolving them in 50% (v/v) methanol, 50 mM preheated sodium acetate buffer, pH 5.8. Solutions of lower concentration were then obtained by dilution in 50 mM sodium acetate buffer, pH 5.8.

2.2. Endo-β-1,4-xylanase (Tx-Xyl) preparation

The thermostable GH11 endo-β-1,4-xylanase (Tx-Xyl) produced by *T. xylanilyticus* was used [28–30]. The native enzyme was produced and purified as previously described [31]. The specific activity of the pure enzyme was 2000 IU/mg protein, where one IU is defined as the amount of endoxylanase required to release 1 μmol of reducing xylose equivalent from birchwood xylan per min at 60 °C.

2.3. Activity assay

Xylanase activity was assayed by monitoring the release of reducing sugars using a colorimetric method [32]. Birchwood xylan (Sigma–Aldrich) (0.5% w/v) was used as substrate in 50 mM sodium acetate, pH 5.8. Measurements were performed by incubating the substrate with appropriately diluted Tx-Xyl aliquot for 10 min at 60 °C in a final volume of 1 mL. At 2 min intervals, samples of 100 μL were removed and mixed with 1.5 mL of Kidby solution (1% Na_2CO_3 and 0.03% potassium hexacyanoferrate [III]). Coloration was developed by heating (at 100 °C) for 5 min, and spectral absorbance was measured at 420 nm. The amount of released sugar was determined using a xylose calibration curve (0–400 μg mL^{-1}). Activity was expressed in terms of International Unit (IU) as defined above.

2.4. Kinetics of inactivation of xylanase by phenolic compounds

The enzyme (Tx-Xyl) (0.5 μM) was incubated with different phenolic compounds at various concentrations (0–1–5–10–20–50–70–80–100 mM) in 50 mM sodium acetate buffer, pH 5.8, in a total volume of 1 mL at 60 °C. Aliquots of 100 μL were withdrawn periodically at 0–5–10–15–30 min, appropriately diluted into buffer and assayed for residual Tx-Xyl activity. The log percent residual activity for each concentration of phenolic compound was plotted versus time. Apparent inactivation rate constants (K_{app}) were obtained from the slopes of these plots, which were then used as a measure of the rates of inactivation (V_i).

Assays and the appropriate controls were carried out in triplicate and average values were considered throughout. Control tests, performed in the absence of phenolic compounds were carried out to determine whether methanol caused inhibition of Tx-Xyl, but no reduction of activity occurred in the presence of methanol (up to 50%, v/v).

Kinetic data analysis of Tx-Xyl inactivation by the several phenolic compounds was done using a sigmoidal V_{imax} (maximal inactivation rate) calculation model. Values of inactivation rates (V_i) at various inhibitor concentrations were fitted to the Hill equation (Eq. (2), see Section 3) using a non linear least-squares regression of SigmaPlot 2000 6.1 (SPSS, USA). The software allowed calculations of the apparent inactivation kinetic parameters (V_{imax} and $K_{0.5}$) and their associated standard errors. The results presented in this paper are average values of triplicate data-sets.

2.5. Analysis of enzyme–phenolic compound interactions using fluorescence spectrophotometry

Steady-state fluorescence analysis was performed on Tx-Xyl samples (5 μM) that had been previously incubated (for 30 min at 60 °C with stirring) with different concentrations of the phenolic compounds (0–1–2.5–5–7.5–10–25–50–100 μM to 1–5–10–20–50–70–80–100 mM) in 50 mM sodium acetate buffer, pH 5.8 (final volume of 1 mL). All fluorescence measurements were made on a SPECTRAmax GEMINI micro-plate spectrophotometer (Molecular Devices Corporation, CA) at 25 ± 1 °C using 0.3 mL standard 96-well black microplates. An excitation wavelength (λ_{exc}) of 295 nm was used to ensure selective excitation of tryptophan residues. Emission spectra were recorded in the range of 320–500 nm using increments of 2 nm. The fluorescence of the phenolic compounds in the buffer was also measured at the same excitation wavelength at the different concentrations employed and used to correct the observed fluorescence prior to further data analysis. The fluorescence quenching processes were studied using the Stern–Volmer theory [33].

3. Results

3.1. Kinetics of the inactivation of Tx-Xyl by phenolic compounds

3.1.1. Inactivation mechanism

The kinetics of inactivation of Tx-Xyl were assessed by incubating the enzyme with different concentrations of various phenolic compounds. At concentrations inferior to 10 mM, no inhibition of Tx-xyl activity was detected. However, at higher concentrations (up to 100 mM), a time- and concentration-dependent loss of enzymatic activity was observed (Fig. 2). For example, at low concentration (20 mM) cinnamic acid reduced Tx-Xyl activity by more than 40% after 30 min, whereas an equivalent loss of activity was observed after 5 min when the concentration of cinnamic acid was 70 mM. At a higher concentration (100 mM), all of the phenolic compounds provoked almost complete enzyme inactivation (≥95% loss of activity after 15 min incubation).

The fact that inhibition is time-dependant precludes competitive inhibition, which is characterized by tight and reversible binding. However, time dependency is consistent with non competitive irreversible inhibition. In this case, inhibition is expected to increase with incubation time, following pseudo-first order kinetics [34,35]. Therefore semi-logarithmic plots of % residual Tx-Xyl activity versus incubation time were prepared. In all cases, these reveal a linear relationship that is consistent with a pseudo-first order inactivation process (Fig. 2). Using Eq. (1) described by Levy [36], it was possible to calculate the apparent pseudo-first order rate constants (K_{app}) from the slopes of the semilogarithmic plots.

$$\mathrm{Log}\left(\frac{[E_a]_t}{[E_a]_0}\right) = -K_{app.}(t) \quad (1)$$

where E_a represents active enzyme and (t) the incubation time.

Afterwards, plotting of the K_{app} values versus phenolic concentrations revealed a saturation behaviour (Fig. 2, insets), indicating that the inhibition process leads to the formation of an inactive Tx-Xyl–phenolic compound complex. However, the plots yielded sigmoidal-shaped curves rather than rectangular hyperbolas that would be typically associated with Michaelis–Menten kinetics. This suggests that more than one phenolic compound molecule binds to one enzyme molecule. According to Monod et al. [37], such sigmoidal inhibition curves can be ascribed to cooperative interaction between inhibitor "binding" sites on the enzyme molecule.

3.1.2. Kinetic inhibition parameters

The non hyperbolic behaviour of plots of K_{app} versus phenolic concentration was confirmed by our failure to fit the data to linear equations, such Lineweaver–Burk or Eadie–Hofstee relationships. Hence, it was impossible to determine the kinetic inhibition parameters V_{imax} (maximal inactivation rate) and K_i using these methods. To access these parameters, the Hill equation (Eq. (2)) was employed. This not only provided V_{imax} and K_i, but also allowed the determination of the degree cooperativity between the inhibitory binding sites.

Assuming that inhibition obeys the following reaction process,

$$E + nI \overset{K}{\rightleftarrows} (E - I_n)$$

then,

$$K = \frac{[E - I_n]}{[E][I]^n}$$

The Hill equation:

$$V_i = \frac{V_{imax} \cdot [I]^n}{K_{0.5}^n + [I]^n} \quad (2)$$

and

$$\log\left(\frac{V_i}{V_{imax} - V_i}\right) = n \ \log[I] - n \ \log \ K_{0.5}$$

where E = free and active enzyme (Tx-Xyl); I = inhibitor (phenolic compound); E–I_n = inactive enzyme–inhibitor complex; n = Hill coefficient that represents apparent number of phenolic compound (inhibitor) molecules reacting with enzyme molecule to form an inactive enzyme complex, with one active site per enzyme molecule K = apparent over-all association constant; $K_{0.5}$ denotes the inhibitor concentration which gives an inactivation rate (V_i) equal to half the maximal inactivation rate (V_{imax}).

Table 1 summarizes the kinetic parameters that characterize the inactivation of Tx-Xyl by the different phenolic compounds. The estimated values for V_{imax} were quite comparable for the five phenolic compounds, although cinnamic acid appeared to induce the fastest inactivation of Tx-Xyl (0.19 min^{-1}). However, the comparison of the apparent association constants revealed that caffeic acid displayed higher $K_{0.5}$ value (90.05 mM) than ferulic acid (79.32 mM), tri-methoxycinnamic acid (75.91 mM), cinnamic acid (72.81 mM) and *p*-coumaric acid (71.29 mM), suggesting that more caffeic acid is involved in the enzyme–inhibitor complex when an inactivation rate equivalent to 50% of V_{imax} is reached. This greater interaction between caffeic acid and Tx-Xyl was further investigated by analyzing the corresponding Hill coefficient (n), an index of binding cooperativity that is dependant both on the number of inhibitor "binding" sites and the strength of the interactions between them. A value of $n = 1$ indicates that binding sites are independent, whereas cooperativity is indicated by a value of $n > 1$, where the integral value is equal to the number of sites. The Hill coefficients presented in Table 1 were derived from the slopes of linear Hill plots (Fig. 3). All values for n were significantly greater than 1, indicating that the binding of the phenolic compounds follows a positive cooperative process. In the case of cinnamic, *p*-coumaric, ferulic and tri-methoxycinnamic acids, the Hill coefficients were close to a value of 3, indicating that at least 3

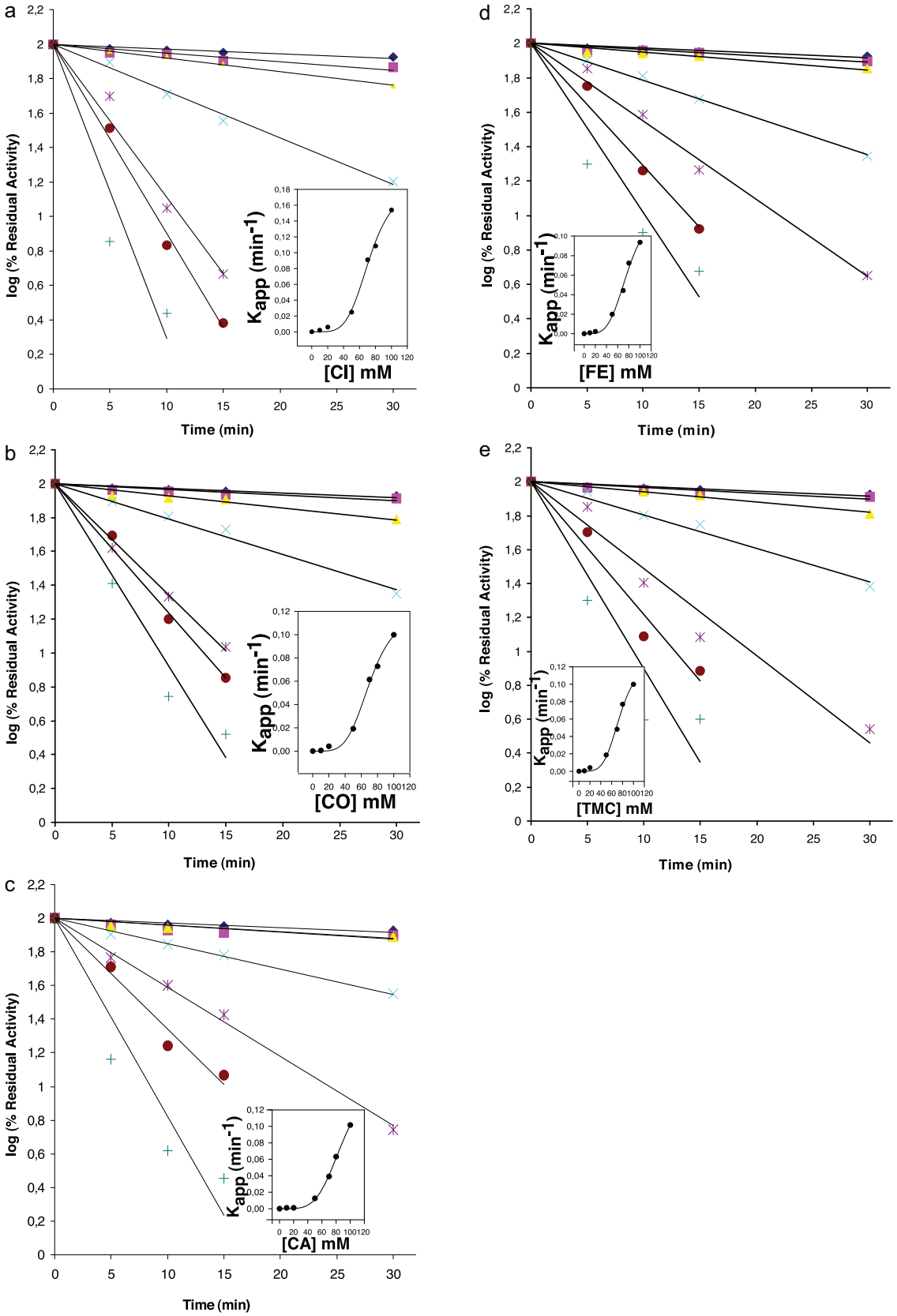

Fig. 2. Kinetics of inactivation of Tx-Xyl by phenolic compounds. Pseudo first-order plots for the inactivation of Tx-Xyl by cinnamic acid (CI) (a), *p*-coumaric acid (CO) (b), caffeic acid (CA) (c), ferulic acid (FE) (d), tri-methoxy-cinnamic acid (TMCI) (e). Tx-Xyl (0,5 μM) was preincubated at 60 °C with 0 mM (◆), 10 mM (■), 20 mM (▲), 50 mM (×), 70 mM (✳), 80 mM (●) and 100 mM (+) of each phenolic compound. Aliquots were withdrawn at indicated time intervals and assessed for residual xylanase activity. Insets: Replots of the apparent pseudo first-order inactivation rate constants (K_{app}) calculated from the main figure as function of phenolic concentration.

Table 1
Kinetic parameters of Tx-Xyl inactivation by phenolic compounds.

	$K_{0.5}$ (mM)	V_{imax} (min^{-1})	Hill coefficient (n)
Cinnamic acid	72.81 ± 4.95	0.19 ± 0.02	2.58
p-Coumaric acid	71.29 ± 4.26	0.12 ± 0.01	2.89
Caffeic acid	90.05 ± 6.13	0.17 ± 0.02	3.43
Ferulic acid	79.32 ± 11.83	0.13 ± 0.03	2.59
3,4,5-Tri-methoxy-cinnamic acid	75.91 ± 7.04	0.13 ± 0.02	2.79

Data (±standard deviation) are mean values of three independent measurements.

molecules bind cooperatively to Tx-Xyl. In contrast, for caffeic acid this value was closer to 4. Accordingly, these results confirm the apparent higher affinity of caffeic acid towards Tx-Xyl.

3.2. Fluorescence study of the interaction of Tx-Xyl with phenolic compounds

3.2.1. Tryptophan fluorescence quenching

To investigate the binding of the phenolic compounds to Tx-Xyl using fluorescence spectroscopy, the fluorescence emission from tryptophan was used, as the fluorescence of the indole chromophore is highly sensitive to its micro-environment making it an ideal choice for reporting protein conformation changes and interactions with other molecules [38,39]. Excitation and emission wavelengths were 295 and 340 nm respectively. In these conditions, the fluorescence emission from cinnamic acid was almost undetectable, while the emission spectra from caffeic, ferulic, *p*-coumaric acids were weak. Only tri-methoxy-cinnamic acid displayed a strong emission, but this reached a maximum at approximately 430 nm (Fig. 4f). Nevertheless, to avoid any data interference, the fluorescence Tx-Xyl titration spectra were corrected with control spectra of phenolic components obtained at the respective concentration.

As depicted in Fig. 4, decreases in the fluorescence intensity of the emission spectra of Tx-Xyl correlated with increases in the concentration of phenolic compounds (from 1 μM to 10 mM), indicating that a concentration-dependant quenching of the intrinsic protein fluorescence had occurred. Maximal quenching was obtained at 10 mM, so emission spectra recorded at higher concentrations (20–100 mM) are not shown. Furthermore, quenching of the fluorescence emission was accompanied by a substantial blue-shift (of 12–14 nm) that reduced the emission maximum from 340 nm to 326–328 nm. Tx-Xyl contains at least 13 tryptophan residues distributed throughout its 182 residues primary sequence, 3 at the surface and 10 embedded in the protein core [28]. Thus, the fluorescence quantum yield of the whole Tx-Xyl macromolecule reflects in reality the mean value of the yields of all 13 tryptophan residues in different environments. The observed phenolic-induced decreases in Tx-Xyl intrinsic fluorescence could result from local protein conformation changes in the bound state, which alter the interactions of some tryptophan residues with neighbouring groups and consequently their emission. Tryptophan fluorescence is, indeed, exquisitely sensitive to position (protein surface or interior) and environment (hydrophobic, polar,. . .) which are in turn directly influenced by the protein conformation. Emission maximum is red-shifted (λ_{max} in the range of 345–355 nm) when tryptophan residues are exposed to a polar environment (exposed to solvent) and have high mobility, while in an apolar environment, tryptophan residues (buried in the protein) display blue-shifted emission (λ_{max} in the range of 325–335 nm) [38,40,41]. A λ_{max} of 320 nm has been reported for free tryptophan in hexane and is considered as typical for buried tryptophan residues in a hydrophobic environment with significant quenching by nearby amino-acid residues. The occurrence of blue shift reveals a selective quenching of solvated tryptophan residues, which emit at longer wavelength and presumably suggests that the interactions between the several phenolic compounds and Tx-Xyl would be mainly surface interactions.

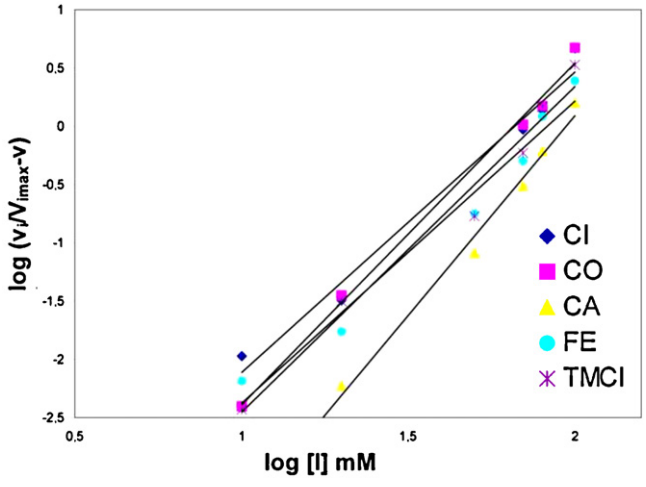

Fig. 3. Hill plots: linear regressions of the plots of log $[V_i/V_{imax} - V)]$ versus log of concentration of cinnamic acid (CI) (◆), *p*-coumaric acid (CO) (■), caffeic acid (CA) (▲), ferulic acid (FE) (●), tri-methoxy-cinnamic acid (TMCI) (✳).

3.2.2. Mechanism of fluorescence quenching

Fluorescence quenching can be dynamic, resulting from collisional encounters between the fluorophore and the quencher, or static resulting from the formation of a non-fluorescent ground state complex between the fluorophore and the quencher. To interpret the data from the fluorescence titration experiments of Tx-Xyl in presence of the phenolic compounds, the Stern–Volmer equation, which can be used to describe both static and dynamic processes, was used:

$$\frac{F_0}{F} = 1 + K_Q \Gamma_0 [Q] = 1 + K_{sv}[Q] \quad (3)$$

where F_0 and F are the fluorescence intensities of Tx-Xyl, recorded at 340 nm (λ_{max} emission), in the absence and presence of quencher, respectively. These data were derived from Tx-Xyl fluorescence titration spectra (Fig. 4). [Q] is the concentration of the quenching agent (i.e. phenolic compounds) and K_{SV} is the Stern–Volmer quenching constant, which can be written as $K_{SV} = K_Q \Gamma_0$, where K_Q is the bimolecular quenching rate constant and Γ_0 is the lifetime of the fluorophore in the absence of quenching agent.

Plots of F_0/F versus [Q], are shown in Fig. 5. These were linear for concentrations ≤1 mM, while a slight downward deviation from linearity was displayed at higher concentrations (>1 mM) (data not shown). This could be explained by the presence of two classes of fluorophore that differentially interact with the quenching agent [42]. The Stern–Volmer quenching constants (K_{SV}) were determined from the slopes of the F_0/F versus [Q] plots, using the linear part (0–1 mM). Considering that the Γ_0 of a bio-molecule is approximately 10^{-8} s [43], the quenching rate constants K_Q were calculated.

As summarized in Table 2, the average K_Q values ranged from $4.33 \times 10^{11}\ M^{-1}\ s^{-1}$ to $10.8 \times 10^{11}\ M^{-1}\ s^{-1}$ for the five phenolic acids. These values are 10- to 100-fold higher than the upper limit value of K_Q associated with a diffusion-controlled bimolecular quenching process involving dynamic quenchers ($\sim 10^{10}\ M^{-1}\ s^{-1}$)

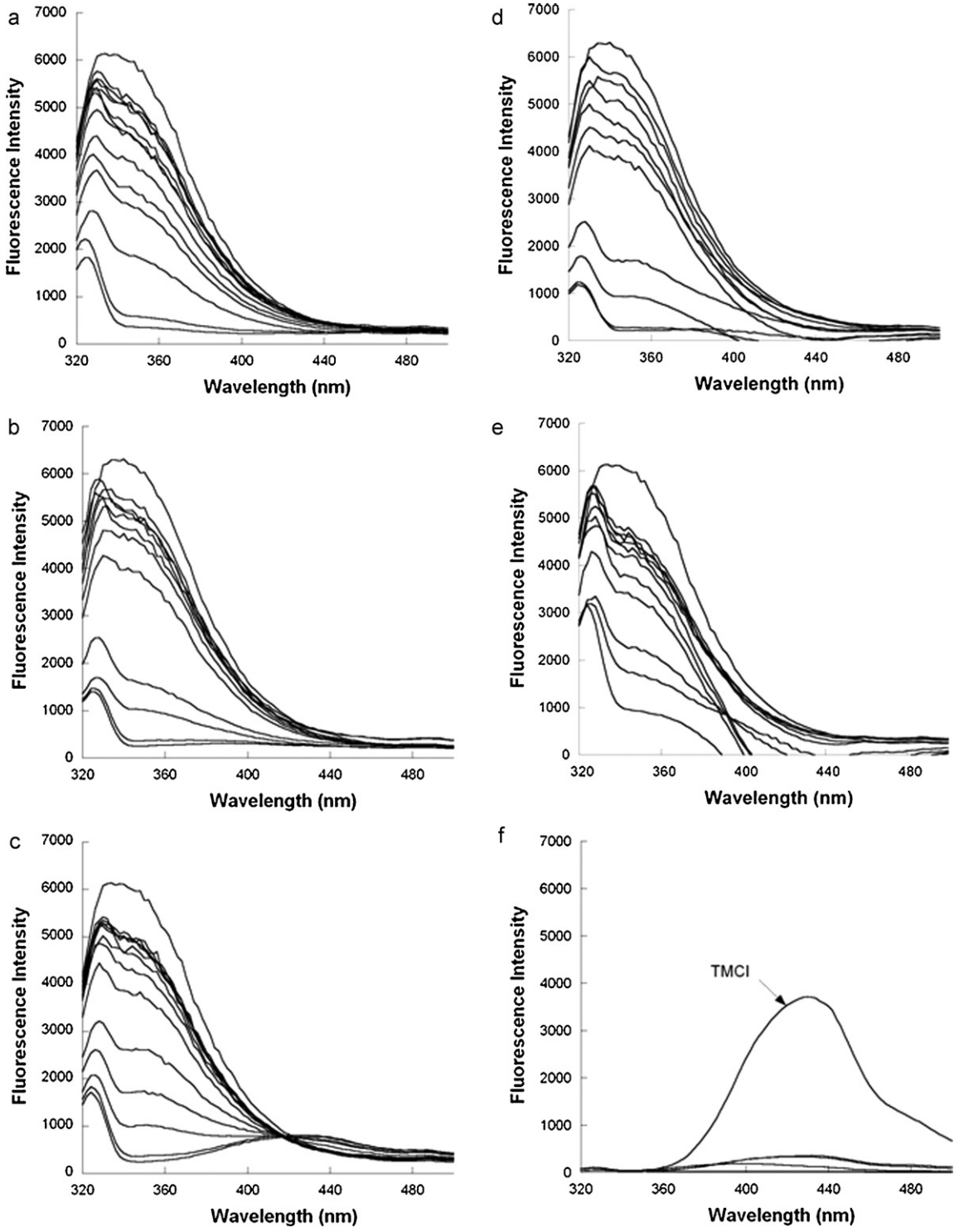

Fig. 4. Representative fluorescence emission spectra of Tx-Xyl (5×10^{-6} M) in the absence and the presence of increasing amounts (from 1×10^{-3} to 10 mM) of cinnamic acid (a), *p*-coumaric acid (b), caffeic acid (c), ferulic acid (d), tri-methoxy-cinnamic acid (e) in 10 mM sodium acetate buffer, pH 5,8 after 30 min of incubation at 60 °C. (f) Control emission spectra of the 5 phenolics (5 mM) (TMCI: tri-methoxy-cinnamic acid). The excitation wavelength was 295 nm. (The fluorescence Tx-Xyl titration spectra are corrected with control spectra of phenolic components obtained at the respective concentration.)

[44]. Therefore, it is unlikely that the quenching of Tx-Xyl is initiated by dynamic collision, but most probably by static quenching through the formation of a complex between Tx-Xyl and the phenolic compounds.

3.2.3. Binding constants

Assuming that the fluorescence quenching of Tx-Xyl was primarily static, it was possible to derive the binding (or affinity) constant (K_A) and from the plot of $\log(F_0 - F)/F$ versus $\log([Q])$, based on the following equation:

$$\log\left(\frac{F_0 - F}{F}\right) = \log \quad K_A + n \quad \log([Q]) \tag{4}$$

Fig. 6 shows the double logarithmic curves obtained for the five phenolic compounds. The plots were almost linear for the whole concentration range (1 μM to 10 mM) and thus allowed

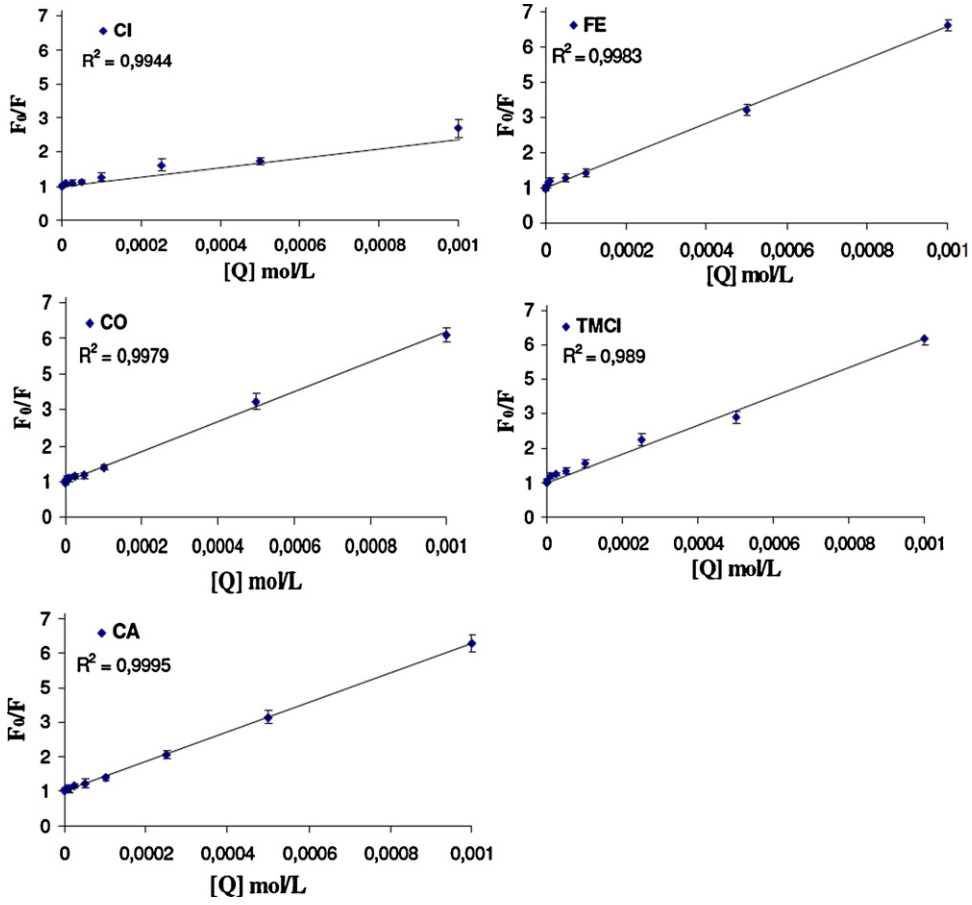

Fig. 5. Stern–Volmer plots of fluorescence quenching of Tx-Xyl treated at 60 °C with different concentrations of cinnamic acid (CI), *p*-coumaric acid (CO), caffeic acid (CA), ferulic acid (FE), tri-methoxy-cinnamic acid (TMCI). λ_{ex} = 295 nm. F_0 and F recorded at λ_{em} = 340 nm. Regression coefficients (R^2).

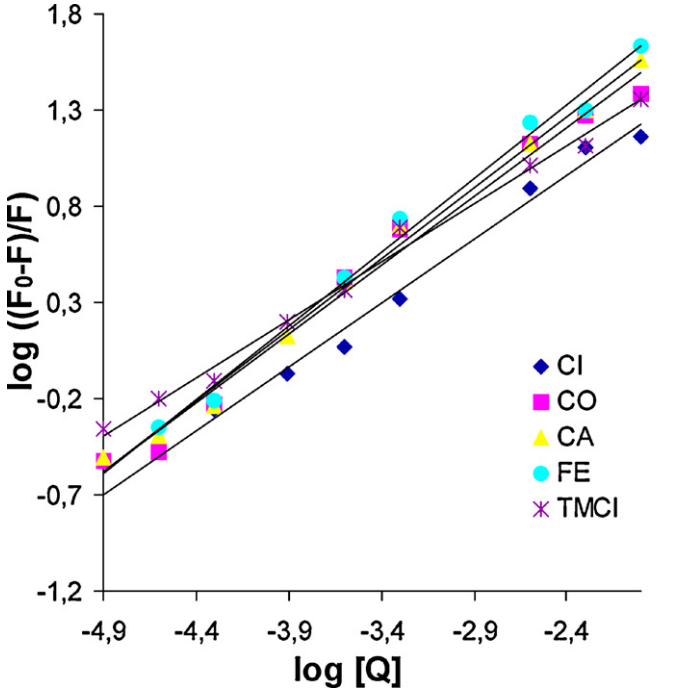

Fig. 6. Logarithmic plots of fluorescence quenching of Tx-Xyl treated at 60 °C with different concentrations (from 1×10^{-3} to 10 mM) of cinnamic acid (CI) (♦), *p*-coumaric acid (CO) (■), caffeic acid (CA) (▲), ferulic acid (FE) (●), tri-methoxy-cinnamic acid (TMCI) (*). Regression coefficients (R) ~0.99. λ_{ex} = 295 nm. F_0 and F recorded at λ_{em} = 340 nm.

calculation of the corresponding K_A and n given in Table 2. Results indicate that Tx-Xyl displays a higher binding affinity for caffeic acid (10.9×10^2 M^{-1}) than for *p*-coumaric acid (8.41×10^2 M^{-1}) and ferulic acid (7.39×10^2 M^{-1}). The lowest affinities were obtained with cinnamic acid (3.60×10^2 M^{-1}) and 3,4,5-tri-methoxy-cinnamic acid (3.61×10^2 M^{-1}). In full agreement with the association constants deduced from the inhibition kinetic study, these results clearly indicate that the affinity of Tx-Xyl increased with the increased hydroxyl group content of the phenolic compounds. Thus, it can be concluded that the presence of aromatic hydroxyl groups plays a rather more important role than the methoxyl groups in the interaction of Tx-Xyl with the phenolic compounds.

The values of binding sites (n) were not considered, since the binding equilibrium given by the double logarithm equation (Eq. (4)) assumes that small quencher molecules bind independently to a set of equivalent and similar binding sites in the protein molecule, and does not take into account any cooperative effect (negative or positive) between the binding sites like it was previously demonstrated by the kinetic approach.

Table 2
Quenching rate constants (K_Q) and binding constants (K_A) of Tx-Xyl to phenolic compounds.

	$K_Q \times 10^{-11}$ (M^{-1} s^{-1})	$K_A \times 10^{-2}$ (M^{-1})
Cinnamic acid	4.33 ± 0.46	3.60 ± 0.29
p-Coumaric acid	9.88 ± 0.94	8.41 ± 1.15
Caffeic acid	10.2 ± 1.00	10.90 ± 0.83
Ferulic acid	10.80 ± 1.04	7.39 ± 0.86
3,4,5-Tri-methoxy-cinnamic acid	9.91 ± 0.73	3.61 ± 0.11

Data (±standard deviation) are mean values of three independent measurements.

4. Discussion

Understanding the interactions of soluble inhibitors that may be generated during biomass pre-treatment with hydrolytic enzymes is an important step towards the optimization of biorefining processes and the enzymes used therein. Two approaches were employed in order to investigate the inactivation mechanism of a xylanase (Tx-Xyl) by several phenolic compounds, which differ with regard to their hydroxyl and methoxyl radical content.

The kinetic analyses demonstrated that inhibition of Tx-Xyl by the different phenolic compounds followed a "multi-site", non competitive inhibition mechanism, indicating that more than one aromatic molecule interacts with the enzyme molecule to induce its complete inactivation. Accordingly, the inhibition of Tx-Xyl by the phenolic compounds does not involve direct interaction with the enzyme active site consistently with the earliest suggestions of Sharma et al. [22]. Indeed, these authors proposed that phenolic compounds could directly affect *in vitro* enzyme activity in two ways: first, by forming a soluble but inactive enzyme–inhibitor complex at low phenolic concentrations, and second by reducing the solubility of enzyme proteins by forming insoluble protein-phenolic complex at high phenolic concentrations [22]. Our kinetic data rather support the formation of inactive enzyme–phenolic complex and confirm the finding of Senior et al. who reported a non competitive inhibition of a xylanase from *T. harzianum* by lignin degradation products generated in spent sulfite pulping liquor [23].

However, a noteworthy aspect of the inhibition mechanism observed for Tx-Xyl is the cooperative effect between multiple binding sites of phenolics. This feature assumes the presence of inter-dependant and interacting phenolic binding sites on the protein molecule with differential affinities. Thus, initial binding of aromatic molecules would occur at high affinity binding sites, which then influence the binding of further inhibitor molecules to other low affinity sites. To some extent, we can consider this as an allosteric behaviour. According to the simplest definition proposed by Taketa el al. [45], allosteric inhibition would be the interaction of an enzyme and an inhibitor at a site on the enzyme that is distinct from the catalytic active site and which results in the loss of enzyme activity. To our knowledge, such an inhibition mechanism has never been described for an enzyme that obeys Michaelien kinetics. Therefore, this observation is no doubt an indication of the quite complex kinetics of catalysis performed by GH11 xylanases.

A characteristic feature of an allosteric inhibition is that loss of enzyme activity is provoked by changes in protein conformation. In the case of Tx-Xyl, such changes are strongly suggested by the significant alterations to the fluorescence emission spectra (blue shift and decrease in the fluorescence quantum yield) that occurred when phenolic compounds bound to the enzyme. Recently, Paes et al. [46] evidenced modest blue-spectral shifts (2.4–3.3 nm) in fluorescence emission spectra of Tx-Xyl when xylotetraose or xylopentaose were bound. These shifts were attributed to the implication of residues tryptophan 7 and/or tyrosine 86 in the interaction [46]. However, in this study the blue shifts induced by the binding of phenolic compounds (notably the blue-shifts of 12–14 nm) are much more significant and cannot be simply attributed to multiple interactions with surface aromatic residues. On the contrary, such large blue shifts are indicative of protein conformational changes [39,47,48] that could affect the micro-environment of internal aromatic residues. Moreover, it is noteworthy that the observed spectral changes occurred at low phenolic compound concentrations (less than 1 mM), whereas the actual inhibition of enzyme activity was only detected at an approximately 10-fold higher concentrations (10 mM). Therefore, it is plausible that subtle protein conformational changes may precede and lead to the loss of enzyme activity. Change in a xylanase three-dimensional structure in presence of lignin black liquor has already been observed by circular dichroïsm [24].

In a broader context, interactions of phenolic compounds with proteins have been largely documented in the literature [49]. Phenolics have been reported to influence biological functions of proteins by altering their physicochemical properties (e.g. solubility, electrophoretical behaviour, hydrophobicity, secondary and tertiary structures, and thermodynamic parameters) [50–53]. The non covalent binding of ferulic acid to human and bovine serum albumins or lysozyme was shown to induce significant changes in protein tertiary structures, while similar interactions of human serum albumin with cinnamic acid, *p*-coumaric acid and caffeic acid were correlated to changes in the secondary structure of the protein [54–56]. Taken together with these data, our results strongly suggest that Tx-Xyl undergoes conformational changes in the presence of phenolic compounds, but further studies (notably circular dichroïsm) will be necessary to validate this hypothesis.

The majority of the interactions of the phenolic compounds with Tx-Xyl are likely to involve residues located at the surface of the enzyme. Indeed, this is implied from the selective quenching of the solvated tryptophan residues. These interactions may include both hydrophobic aromatic ring stacking (between phenolic compounds and tryptophanyl side chains) and/or hydrogen interactions between their (COOH, OH) functional groups and the basic amino acid residues. The elucidation of the relative importance of the two types of interaction requires further detailed studies. However, the presence of approximately 11 surface-exposed hydrophobic patches on Tx-Xyl macromolecule may constitute potential phenolic binding sites [28]. Otherwise, mobility of the thumb-like loop of Tx-Xyl has been reported as a key factor in the catalysis since precise positioning of this loop will determine the width of the catalytic cleft [46]. Therefore, stacking interactions with tryptophan residues located in the vicinity of the thumb-like loop of Tx-Xyl (e.g. Trp 109) would affect the thumb mobility, which would hinder the correct operation of the catalytic events (substrate selectivity and docking, accommodation of the xylan polymer into the catalytic cleft and finally cleavage of the glycosidic bound) and would thus result in the loss of the enzyme activity [57].

With regards to the role of phenolic functional groups in the inhibitory interactions, although all five phenolic compounds displayed rather similar and comparable inhibitory effects on Tx-Xyl activity, the association constants deduced from the kinetic study and the fluorescence analysis clearly indicate that caffeic acid has a higher interaction affinity for Tx-Xyl. Thus, an apparent correlation between the hydroxyl (OH) content of the phenolic compounds and inhibitory potency can be established. In contrast, no equivalent correlation can be derived for the methoxyl radicals, since results obtained for the 3,4,5-tri-methoxy-cinnamic acid are rather similar to those of cinnamic acid. Recently, Pan has drawn highly similar conclusions regarding the impacts of various lignin samples on the action of cellulase cocktail [26]. Indeed, by chemically modifying (hydroxypropylation) the phenolic hydroxyl groups of lignins, the author showed that it is possible to diminish the inhibitory effects of lignins on cellulases. This evidence reinforces a significant *corpus* of information that pinpoints phenolic hydroxyl groups as key mediators of lignin–enzyme interactions. Moreover, beyond enzymes, it is known that phenolic hydroxyl groups are necessary and important for the adsorption of tannins and lignins by proteins [58], mediating interactions between nucleophilic sites of proteins and the quinone methide groups of lignins [59].

5. Conclusions

Biomass-degrading enzymes display rather diverse structures and properties. Likewise, the chemical diversity of lignin

degradation products is very extensive. Therefore, it is impossible to draw from any one study general conclusions about the effects of soluble phenolic compounds on enzymes. Nevertheless, the work presented here contributes to the overall understanding of the interactions between a GH11 endo-xylanase and soluble inhibitors (phenolic monomers, oligomers,. . .) that may be generated during biomass pre-treatment. Notably, results pinpoint the importance of surface interactions and the implications of the hydroxyl (OH) content in the inhibitory effects.

The better understanding of the factors that mediate interactions between soluble phenolic compounds or lignins and biomass degrading enzymes will contribute to the rational design of better biorefining processes, notably through the improvement of pretreatment. Obvious improvements will include the development of strategies that will limit the formation of hydroxyl-bearing phenolic compounds; the specific low-cost detoxification of pretreated biomass before enzymatic processing [60] and finally the selection or engineering of enzymes [61] that are weakly or/not inhibited by phenolics.

Acknowledgements

The authors gratefully acknowledge the region Champagne-Ardenne (France) for the financial support of the PhD position of I. Boukari and Dr. G. Paës (Inra, UMR FARE) for fruitful discussion on the thumb mobility in Tx-Xyl.

References

[1] C.A. Cardona, Ó.J. Sánchez, Bioresour. Technol. 98 (2007) 2415–2457.
[2] S.T. Merino, J. Cherry, Biofuels 108 (2007) 95–120.
[3] Y. Lin, S. Tanaka, Appl. Microbiol. Biotechnol. 69 (2006) 627–642.
[4] Y. Sun, J. Cheng, Bioresour. Technol. 83 (2002) 1–11.
[5] R. Kumar, S. Singh, O. Singh, J. Ind. Microbiol. Biotechnol. 35 (2008) 377–391.
[6] D.E. Akin, Biofpr 2 (2008) 288–303.
[7] R.P. Chandra, R. Bura, W.E. Mabee, A. Berlin, X. Pan, J.N. Saddler, Adv. Biochem. Eng. Biotechnol. 108 (2007) 67–93.
[8] A.T.W.M. Hendriks, G. Zeeman, Bioresour. Technol. 100 (2009) 10–18.
[9] M.A. Kabel, G. Bos, J. Zeevalking, A.G.J. Voragen, H.A. Schols, Bioresour. Technol. 98 (2007) 2034–2042.
[10] S. Larsson, E. Palmqvist, B. Hahn-Hägerdal, C. Tengborg, K. Stenberg, G. Zacchi, N.-O. Nilvebrant, Enzyme Microb. Technol. 24 (1999) 151–159.
[11] M. Mes-Hartree, J.N. Saddler, Biotechnol. Lett. 5 (1983) 531–536.
[12] E. Palmqvist, B. Hahn-Hägerdal, M. Galbe, G. Zacchi, Enzyme Microb. Technol. 19 (1996) 470–476.
[13] E. Palmqvist, B. Hahn-Hagerdal, Bioresour. Technol. 74 (2000) 25–33.
[14] E. Ximenes, Y. Kim, N. Mosier, B. Dien, M. Ladisch, Enzyme Microb. Technol. 46 (2010) 170–176.
[15] Y.H. Zhang, J. Ind. Microbiol. Biotechnol. 35 (2008) 367–375.
[16] M. Kleinert, T. Barth, Chem. Eng. Technol. 31 (2008) 736–745.
[17] M. Cantarella, L. Cantarella, A. Gallifuoco, A. Spera, F. Alfani, Biotechnol. Prog. 20 (2004) 200–206.
[18] D.B. Hodge, M.N. Karim, D.J. Schell, J.D. McMillan, Bioresour. Technol. 99 (2008) 8940–8948.
[19] J.J. Ko, Y. Shimizu, K. Ikeda, S.K. Kim, C.H. Park, S. Matsui, Bioresour. Technol. 100 (2009) 1622–1627.
[20] K. Freudenberg, Science 148 (1965) 595–600.
[21] J. Ralph, G. Brunow, W. Boerjan, Encyclopedia of Life Sciences Copyright © 2007, John Wiley & Sons, 2007, 1–10.
[22] A. Sharma, O. Milstein, Y. Vered, J. Gressel, H.M. Flowers, Biotechnol. Bioeng. 27 (1985) 1095–1101.
[23] D.J. Senior, P.R. Mayers, C. Breuil, J.N. Saddler, in: T.K. Kirk, H.-M. Chang (Eds.), Biotechnology in Pulp and Paper Manufacture, Butterworth-Heinemann, Boston, MA, 1990, pp. 169–182.
[24] F. Kaya, J.A. Heitmann, T.W. Joyce, J. Biotechnol. 80 (2000) 241–247.
[25] C. Tengborg, M. Galbe, G. Zacchi, Enzyme Microb. Technol. 28 (2001) 835–844.
[26] X. Pan, J. Biobased Mater. Bioenergy 2 (2008) 25–32.
[27] V.J.H. Sewalt, W.G. Glasser, K.A. Beauchemin, J. Agric. Food Chem. 45 (1997) 1823–1828.
[28] G.W. Harris, R.W. Pickersgill, I. Connerton, P. Debeire, J.-P. Touzel, C. Breton, S. Pérez, Proteins 29 (1997) 77–86.
[29] E. Samain, P. Debeire, J.P. Touzel, J. Biotechnol. 58 (1997) 71–78.
[30] J. Touzel, M. O'Donohue, P. Debeire, E. Samain, C. Breton, Int. J. Syst. Evol. Microbiol. 50 (2000) 315–320.
[31] M. Debeire-Gosselin, M. Loonis, E. Samain, P. Debeire, in: J. Visser, G. Beldman, M.A. Kusters-van Someren, A.G.J. Voragen (Eds.), Xylans and Xylanases, Elsevier Science Publishers, 1992, pp. 463–466.
[32] D. Kidby, D. Davidson, Anal. Biochem. 55 (1973) 321–325.
[33] V.O. Stern, M. Volmer, Phys. Zeitschr. 20 (1919) 183–188.
[34] S.L. Hazen, L.A. Zupan, R.H. Weiss, D.P. Getman, R.W. Gross, J. Biol. Chem. 266 (1991) 7227–7232.
[35] F. Renosto, P.A. Seubert, P. Knudson, I.H. Segel, J. Biol. Chem. 260 (1985) 11903–11913.
[36] H.M. Levy, P.D. Leber, E.M. Ryan, J. Biol. Chem. 238 (1963) 3654–3659.
[37] J. Monod, J. Wyman, J.P. Changeux, J. Mol. Biol. 12 (1965) 88–118.
[38] M.R. Eftink, Methods Biochem. Anal. 35 (1991) 127–205.
[39] Y. Engelborghs, J. Fluoresc. 13 (2003) 9–16.
[40] M.R. Eftink, C.A. Ghiron, Biochemistry 15 (1976) 672–680.
[41] J.T. Vivian, P.R. Callis, Biophys. J. 80 (2001) 2093–2109.
[42] S.S. Lehrer, P.C. Leavis, Methods Enzymol. 49 (1978) 222–236.
[43] G. Valensin, T. Kushnir, G. Navon, J. Magn. Reson. 46 (1982) 23–29.
[44] W.R. Ware, J. Phys. Chem. 66 (1962) 455–458.
[45] K. Taketa, B.M. Pogell, J. Biol. Chem. 240 (1965) 651–662.
[46] G. Paes, V. Tran, M. Takahashi, I. Boukari, M.J. O'Donohue, Protein Eng. Des. Sel. 20 (2007) 15–23.
[47] M.R. Eftink, C.A. Ghiron, J. Phys. Chem. 80 (1976) 486–493.
[48] M.R. Eftink, C.A. Ghiron, Anal. Biochem. 114 (1981) 199–227.
[49] N. Balasundram, K. Sundram, S. Samman, Food Chem. 99 (2006) 191–203.
[50] J. Kang, Y. Liu, M. Xie, S. Li, M. Jiang, Y. Wang, BBA-Gen Subjects 1674 (2004) 205–214.
[51] H.M. Rawel, S.K. Frey, K. Meidtner, J. Kroll, F.J. Schweigert, Mol. Nutr. Food Res. 50 (2006) 705–713.
[52] H.M. Rawel, S. Rohn, H.-P. Kruse, J. Kroll, Food Chem. 78 (2002) 443–455.
[53] S. Rohn, H.M. Rawel, J. Kroll, J. Agric. Food Chem. 50 (2002) 3566–3571.
[54] H.M. Rawel, K. Meidtner, J. Kroll, J. Agric. Food Chem. 53 (2005) 4228–4235.
[55] J. Min, X. Meng-Xia, Z. Dong, L. Yuan, L. Xiao-Yu, C. Xing, J. Mol. Struct. 692 (2004) 71–80.
[56] Y. Zhang, Y. Yue, J. Li, X. Chen, J. Photochem. Photobiol. B 90 (2008) 141–151.
[57] P. Biely, M. Vrsanská, M. Tenkanen, D. Kluepfel, J. Biotechnol. 57 (1997) 151–166.
[58] H. Kawamoto, F. Nakatsubo, K. Murakami, Mokuzai Gakkaishi 38 (1992) 81–84.
[59] V.J.H. Sewalt, W.G. Glasser, J.P. Fontenot, V.G. Allen, J. Sci. Food Agric. 71 (1996) 195–203.
[60] S.I. Mussatto, I.C. Roberto, Bioresour. Technol. 93 (2004) 1–10.
[61] A. Berlin, N. Gilkes, A. Kurabi, R. Bura, M.B. Tu, D. Kilburn, J. Saddler, Appl. Biochem. Biotechnol. 121 (2005) 163–170.